Indian Journal of Chemistry
Vol. 47A, June 2008, pp. 836-842

Synthesis, characterization and kinetic studies on complex formed between amantadine hydrochloride and sodium molybdate at physiological *p*H

N Sridevi* & K K Mohammed Yusuff

Department of Applied Chemistry, Cochin University of Science and Technology, Kochi, Kerala, 682 022, India
Email: sritatavarti@gmail.com

Received 6 February 2007; revised 12 May 2008

The title reaction was undertaken to establish the interaction between amantadine and molybdate at physiological *p*H. Identical FTIR spectra, TG-DTA curves and CHN data of the complexes formed from three solutions at *p*H 1.5, 7.4 and 8.0 indicate that the same complex was formed at all the three *p*Hs. The FTIR spectrum shows shift in peaks corresponding to primary amino group of the drug due to coordination to molybdate. An octahedral geometry is assigned to the complex. The kinetics of the complexation has been studied at low concentrations of the reactants using UV-visible spectrophotometry. At *p*H 7.4, the initial rate varies linearly with [molybdate]. A plot of initial rate versus [drug] is linear passing through origin. These results indicate that the drug and molybdate react at *p*H 7.4 even at low concentrations. At *p*H 1.5, the rate increases linearly with increase in [drug] but decreases with [molybdate]. The effect of *p*H and ionic strength on the rate of the reaction has also been studied. A suitable mechanism has been proposed for the reaction. Reaction between the drug and molybdate even at low concentrations and the fact that the amino group of amantadine required to be free for its function as antiviral, is bound to molybdate in the complex suggests that simultaneous administration of the drug and molybdate supplements should be avoided.

IPC Code: Int. Cl.[8] C07F11/00

Amantadine hydrochloride (1-adamantanamine hydrochloride, tricyclo[3.3.1.1^{3,7}]dec-1-ylamine hydrochloride or L-adamantanamine) is used widely to treat influenza A and parkinsonism[1]. Molybdenum is a component of the enzymes xanthine oxidase, sulfite oxidase, and aldehyde oxidase[2]. Its supplementation may be necessary in people undergoing rapid weight loss or in those with malnutrition [3]. Molybdenum salts commonly used as supplements are ammonium molybdate and sodium molybdate [4]. Several metal complexes of amantadine are reported in literature in the recent past. Complex formation with iron(III) at *p*H 3 has been reported by Mustafa, Ahmed A *et al.*[5]. Complexes of Pt(II) have been reported by Tang, Wenxia *et al.*[6] while other polyoxometalates containing Ce, W, Pr, Ni, V and Mn were reported by Liu Shu-Xia and others[7]. Compounds of molybdenum and amantadine with the formulae, $(C_{10}H_{18}N)_5PMo_{12}O_{40}Cl_2.5H_2O$ (ref. 8), $(C_{10}H_{18}N)_6\ As_2Mo_{18}O_{62}.6CH_3CN.6H_2O$ (ref. 8), $(C_{10}H_{18}N)_4Mo_8O_{26}.6(CH_3)_2SO$ (ref. 9) and trans-$(AdNH)_2Mo(OSiMe_3)_4$ (ref. 10) have also been reported. All the amantadine containing molybdenum compounds reported so far have been prepared under non physiological *p*H conditions, often in the presence of organic solvents and therefore it is not clear if amantadine reacts with molybdate under physiological conditions also. The absorption of a drug through gastrointestinal tract is dependent on its physical properties like solubility in water, size and ionic nature which in turn are dependent on the *p*H of the medium[11-13]. Since only the free and unchanged drug can function at the active site in the body, if molybdate reacts with amantadine when the two are administered together, the solubility or chemical form of the drug and hence its absorption and function can be affected. The title investigation was therefore taken up to verify the reaction between molybdate and amantadine at physiological conditions. The *p*H values chosen for this study are 1.5, 7.4 and 8.0, since a *p*H of 1 – 2 exists in stomach and a *p*H of 7.4 is maintained in blood and other organs and tissues. Under diseased condition, the *p*H of some *p*arts of the body may rise up to 8.0.

Materials and Methods

The *p*H of the solutions was adjusted either with hydrochloric acid or tris buffer. Analytical grade hydrochloric acid, tris buffer, amantadine hydrochloride and sodium molybdate dihydrate were used as obtained. All solutions were prepared in doubly distilled water. The stock drug solutions were

prepared afresh before each set of runs and the remaining solutions were prepared once in a week.

To check the occurrence of reaction, mixtures of molybdate and the drug were prepared quantitatively at the desired *p*H and their UV-visible absorption spectra, were obtained in the range 200-800 nm (Thermo Electron Corporation, Evolution 300), against a suitable reference solution. The spectrum of the drug without metal ions (drug blank) and that of the metal ion without drug (metal blank) in the same solvent as that used in the reaction mixtures were also measured separately using the same concentrations. Since absorbance is additive, in the absence of a reaction the absorbance of the reaction mixture at each wavelength should be equal to the sum of the absorbances of the metal and drug blanks at that wavelength. Any difference in these values indicates interaction. This was verified over the entire spectral range scanned. The software, Microsoft Excel (MS Office XP, Microsoft, USA) was used for this purpose. The samples were also screened for any visible precipitation or turbidity. The concentration of the metal ion and drug in the reaction mixtures was varied near to that obtained by dissolving one commercial tablet in 200 ml.

Synthesis and characterization of amantadine-molybdate complex

To prepare the drug-molybdate complex, about 0.1 g of amantadine hydrochloride was dissolved in 40 ml of water. The *p*H of the solution was adjusted to the required value using 5 ml of dil. HCl or tris-buffers and 2.8 g of sodium molybdate dihydrate dissolved in 5 ml water was added. The precipitate resulting was washed several times with water and dried over vacuuo. The yield of the product was nearly 0.1 g at all the three *p*Hs. FTIR spectra were obtained as KBr pellets (Jasco 4100). CHN analysis was carried out on an Elementar Vario EL III CHN analyser (STIC, Kochi, India). TG-DTA curves of the sample were obtained (Diamond, Perkin-Elmer) in the range 38-1000°C at a heating rate of 10°C/min in nitrogen atmosphere (2 bar).

Kinetic studies

All kinetic runs were carried out at 28°C and at a constant ionic strength of 0.1 mol dm^{-3}, maintained using sodium chloride, unless otherwise mentioned. A constant concentration of tris-buffer was used in all kinetic runs carried out in the vicinity of *p*H 7.4. The reaction was initiated with amantadine and the progress of the reaction was monitored by following the absorbance of molybdate at a wavelength of 223 nm in acid medium and at 250 nm in tris buffers. The speed of the reaction was assessed by initial rate method. The initial rates were obtained by fitting the concentration versus time data into a second order polynomial and obtaining the slope of the polynomial at zero time. This was done using the software Microcal Origin (Ver 3.54, Microcal Software Inc. USA) and Microsoft Excel (MS Office XP, Microsoft, USA). The initial rates were reproducible within an error of ± 10%.

Results and Discussion

After about 18 hours of mixing, the UV-visible absorption spectra of mixtures of amantadine and sodium molybdate, prepared at *p*H 1.5 showed lowering of absorption in some regions and elevation in other regions when compared with the expected spectrum computed from the individual spectra of the two (Fig. 1), showing chemical interaction between amantadine and molybdate ion. Similar result was observed at *p*H 7.4 as well as 8.0.

At high concentrations of sodium molybdate and the drug, a white substance separated from solutions at all the three *p*H values employed. CHN and metal analysis data, TG-DTA curves, and FTIR spectra of the three precipitates were identical, within the limits of experimental error, indicating that the substance obtained from the three different media was identical.

The C, H and N percentages of the samples are about 50.1-51.15, 7.76-7.88 and 6.05-6.26 respectively. This corresponded to an atomic ratio of 10:18:1 for

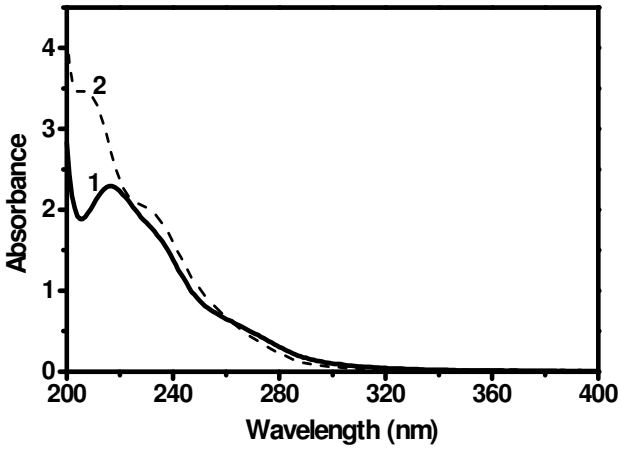

Fig. 1—UV-visible absorption spectra of amantadine molybdate complex. [1, observed spectrum of mixture of amantadine and molybdate; and, 2, expected spectrum of mixture amantadine and molybdate].

carbon, hydrogen and nitrogen, in agreement with the molecular formula of amantadine and shows that no oxidation of amantadine has taken place. The molybdenum content of the sample was found to be 19.5-20.1%. Thus, the elemental analysis data suggested an empirical formula, $(C_{10}H_{17}N)_2H_2MoO_4$ for the complex. In neutral and alkaline medium, molybdate exists as monomeric MoO_4^{2-}. In acid medium, it is protonated and various polymeric species result from the protonated molybdate, the predominant polymeric forms being, $Mo_7O_{25}^{6-}$ and $Mo_8O_{26}^{4-}$ (ref. 14). Formation of the polymeric species is negligible when molybdate concentration is less than 1.0×10^{-3} mol dm^{-3} (ref. 15). Further, the protonation of tetrahedral molybdate in acid medium is kinetically slow and results in an octahedral species[16]. We carried out the complexation by mixing freshly prepared molybdate with amantadine chloride present at the required *p*H. From the CHN data of the complex it is obvious that the monomeric molybdate ion precipitated amantadine from the solutions of *p*H 1.5 as well as higher. On the other hand, earlier Juan Li *et al*.[9] prepared a polyoxymetallate between molybdenum and amantadine by mixing amantadine with a solution of molybdate previously acidified to about 2 mol dm^{-3} HCl, such that it existed predominantly in polymeric form at the time of complexation. They recrystallized their pink coloured product from DMSO, and reported the formula, $(C_{10}H_{18}N)_4Mo_8O_{26}\cdot 6(CH_3)_2SO$ for the same. From the CHN data we obtained for our white complex, it is clear that the molybdenum-amantadine complex formed in weakly acidic solutions is different from that reported by Juan Li *et al*. Moreover, our complex was completely insoluble in DMSO.

There are two ways in which amantadine can be associated to the molybdate ion. It may be bound to the metal ion either through N–H--O-Mo bonds, without actual coordination to the metal ion, or through a direct coordination to the metal ion by the amino nitrogen. In the former process, the molybdate ion remains in the tetrahedral geometry while the latter process involves expansion of coordination around the metal ion and hence conversion of the tetrahedral molybdate to octahedral species. We obtained FTIR spectral and kinetic evidence for the latter process.

FTIR spectra of the complex and that of pure amantadine hydrochloride (AMN) were obtained in the region 400-4000 cm^{-1}. The spectrum of pure amantadine hydrochloride was identical to that reported in literature [17,18]. Upon comparing the FTIR spectrum of the sample with that of AMN, it was noticed that the peaks observed in pure AMN (Fig. 2A) at 1500 and 1605 cm^{-1} correspond to N–H bend shift to 1542 and 1616 cm^{-1}, respectively, in the complex (Fig. 2B), and the peak at 1085 cm^{-1} corresponding to C–N bend shifts to 1092 cm^{-1}. The C–H stretching of AMN results in a broad doublet with peaks at 2924 and 2852 cm^{-1} in the pure ligand. The N-H stretching band of the aliphatic amino group expected for amantadine in the region 2961 to 3087 cm^{-1} by Pierre D. Harvey and others[18] was observed in pure AMN at 3038 cm^{-1}. This peak shifts to 2896 cm^{-1} upon complexation. In the complex, the peak at 2852 cm^{-1} corresponding to C–H stretching was observed at the same position and the peak expected at 2924 cm^{-1} also appeared at the same position but as a weak shoulder to the N–H stretching peak at 2896 cm^{-1}. It is known that the bending modes of amine N–H and C–N bonds shift to higher frequencies while the N–H stretching frequency shifts to lower frequencies upon coordination to a metal ion[19] commensurate with the shifts observed in the present case. Thus it may be inferred that amantadine was strongly bound to molybdate ion through direct coordination through the primary amine group. It is important to note that Juan Li *et al*.[9] did not notice any changes in the IR spectrum of amantadine upon reacting with molybdate in 2 mol dm^{-3} acid, as the amino nitrogen of the drug was bound only through hydrogen bridges to the oxygen atoms in their compound. Further, formation of an N–H--O–Mo bond is expected to cause a broadening of the IR peaks corresponding to the N–H bond and appearance of O-H peak, which was not observed for our

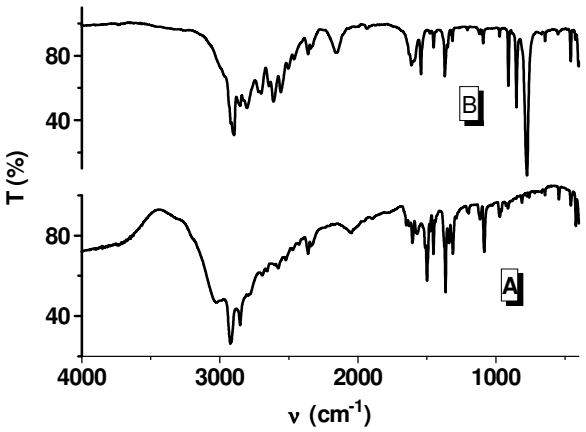

Fig. 2—FTIR spectra of pure amantadine hydrochloride (A), and, amantadine molybdate complex (B).

complex. This confirms that, in the complex formed in the present study, the amino nitrogen of the ligand coordinates directly to the metal ion causing conversion of the tetrahedral species to octahedral. This result is significant in view of the fact that the function of amantadine as an antiviral depends on hydrogen-bonded interactions between histidine residue of the M2 protein of the Influenza A virus and the ammino group of the amantadine[21,22]. Further, the peaks corresponding to molybdate ion appears in the complex under study at 853 and 910 cm^{-1} and an additional very strong peak was observed at 778 cm^{-1}, which is not known for pure molybdate ion. This new peak is probably due to Mo–N–H rocking frequency.

The thermogram of the sample obtained in nitrogen between 38-1000°C is shown in Fig. 3 along with that of pure amantadine hydrochloride. Pure amantadine hydrochloride exhibits a single weight loss region in the temperature region 190-300°C. Unlike pure amantadine, the organic part of the present sample was lost in three stages: the first at about 180-250, second one at 250-395 and the third one at 395-435°C probably due to formation of intermediate compounds with molybdate. This confirms that amantadine complexes with molybdate. The intermediates formed could not be identified due to overlap of the weight loss regions. However, an intermediate of the form $MoO_4(NH_3)_2$ may be envisaged to have formed. The weight of the sample at 435°C was consistent with formation of MoO_3 upon complete loss of the organic part. The sample showed another weight loss in the region 670-770°C and the weight of the sample at 770°C was less than what may be expected if MoO was formed. This may be due to sublimation of MoO_3 above 750°C.

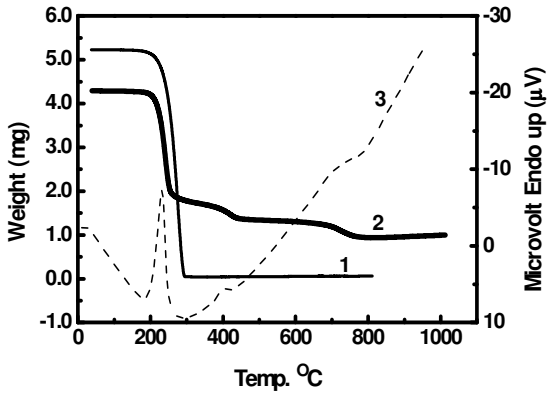

Fig. 3—TG-DTA curves. [1, TG curve of pure amantadine hydrochloride; 2, TG curve of amantadine molybdate synthesized at *p*H 7.4; and, 3, DTA curve of amantadine molybdate synthesized at *p*H 7.4].

Attempts to grow a single crystal of the complex were futile as the complex did not dissolve in any of the commonly used solvents including complexing solvents like DMSO and DMF.

The synthesis and characterization studies confirmed that amantadine reacted with molybdate at all the three *p*Hs at high concentrations. However, in order to draw conclusions regarding their *in vivo* interaction, it is essential to confirm that the reaction persists at low concentrations also. We therefore studied the kinetics of reaction of amantadine with molybdate at *p*H 1.5 and 7.4 employing low concentrations of amantadine and sodium molybdate, the results of which are presented in Table 1.

Table 1—Initial rates obtained at varying concentrations of the drug and metal ion at 28°C

*p*H	[Amantadine] $\times 10^3$ (mol dm^{-3})	[Molybdate] $\times 10^5$ (mol dm^{-3})	Ionic strength $\mu \times 10$	Initial rate $\times 10^{10}$ (mol $dm^{-3} s^{-1}$)
1.5	2.1	10.0	1.0	-11.1
1.5	4.3	10.0	1.0	-8.7
1.5	5.3	10.0	1.0	-7.3
1.5	6.4	10.0	1.0	-5.1
1.5	7.5	10.0	1.0	-3.8
1.5	8.5	10.0	1.0	-3.2
1.5	10.7	10.0	1.0	-0.5
1.5	5.3	0.5	1.0	-4.5
1.5	5.3	1.0	1.0	-4.6
1.5	5.3	3.0	1.0	-5.5
1.5	5.3	5.0	1.0	-6.1
1.5	5.3	10.0	1.0	-7.3
1.5	5.3	30.0	1.0	-13.6
1.0	5.3	3.0	1.0	-3.5
1.2	5.3	3.0	1.0	-3.8
1.4	5.3	3.0	1.0	-4.8
1.6	5.3	3.0	1.0	-6.2
1.8	5.3	3.0	1.0	-8.7
2.0	5.3	3.0	1.0	-11.8
1.5	5.3	1.0	0.3	-8.8
1.5	5.3	1.0	2.7	-4.1
1.5	5.3	1.0	3.3	-3.0
1.5	5.3	1.0	4.3	-2.8
1.5	5.3	1.0	5.3	-2.6
7.4	1.1	10.0	1.0	1.7
7.4	2.1	10.0	1.0	3.7
7.4	3.2	10.0	1.0	5.5
7.4	4.3	10.0	1.0	7.0
7.4	5.3	10.0	1.0	8.5
7.4	5.3	0.5	1.0	-17.8
7.4	5.3	1.0	1.0	-15.8
7.4	5.3	2.0	1.0	-13.4
7.4	5.3	3.0	1.0	-11.3
7.4	5.3	5.0	1.0	-6.3
7.4	5.3	10.0	1.0	8.5
7.0	5.3	1.0	1.0	-14.2
7.2	5.3	1.0	1.0	-15.6
7.6	5.3	1.0	1.0	-18.0
7.8	5.3	1.0	1.0	-22.9
8.0	5.3	1.0	1.0	-28.3

At *p*H 7.4, a change in the absorbance with time was noticed when amantadine was added to molybdate indicating that the reaction between molybdate and drug was not completed immediately upon mixing the two. At a constant [molybdate] of 1.0×10^{-4} mol dm^{-3}, the initial rate of the reaction was positive and increased further when amantadine concentration was varied in the range $1.0 - 5.3 \times 10^{-3}$ (Table 1). A plot of initial rate against [amantadine] was found to be linear passing through origin (r = 0.998) indicating first order with respect to amantadine. On the other hand, the initial rate of reaction was found to be negative at low molybdate concentrations and became progressively less negative when the initial [molybdate] was varied from $0.5 - 10.0 \times 10^{-5}$ mol dm^{-3} at constant [amantadine]. The initial rate became positive at a molybdate concentration of 1.0×10^{-4} mol dm^{-3}. The positive rate can be attributed to formation of aggregates and corresponding increase in absorbance, in the absence of which the reaction would show a decrease in absorbance of molybdate and hence a negative rate. Although the rate of change of absorbance of molybdate varied with amantadine indicating interaction with molybdate, the initial absorbance of reaction mixtures obeyed Beer-Lambert's law at both *p*H, when molybdate was varied in the presence of constant [amantadine]. This confirmed that the complexation was not complete immediately upon mixing the reactants. A plot of initial rate against initial [molybdate] was found to be linear with an intercept on the rate axis (r = 0.998), suggesting first order with respect to molybdate. The intercept on the negative rate axis indicates that at very low concentrations of molybdate, the rate became more negative with increase in [molybdate] and showed a different dependence on molybdate. This matter could not be pursued further due to low absorbance of molybdate at lower concentrations than that employed in the present study. These studies indicate that the reaction between amantadine and molybdate involved both the reactants in the rate determining step. The effect of *p*H on the rate of the reaction was studied in the range 7.0-8.0. The rate became more negative with increase in *p*H and a plot of $1/[H^+]$ versus initial rate was linear with an intercept (r = 0.994). In this *p*H range molybdate exists exclusively as MoO_4^{2-}. The pK_a and percentage ionized at *p*H 7.4 of amantadine are 10.14 at 37°C and 97.5%, respectively[23,24]. The observed *p*H effect indicates that the neutral $C_{10}H_{17}N$ is the predominant reactive species, in spite of its low concentration. Change in ionic strength of the medium did not exhibit any effect on the reaction confirming this. Thus the mechanism of reaction at *p*H 7.4 may be given as shown in Scheme 1.

$$C_{10}H_{18}N^+ \overset{K_a}{\Leftrightarrow} C_{10}H_{17}N + H^+ \quad \ldots (1)$$

$$C_{10}H_{17}N + MoO_4^{2-} \xrightarrow[(\text{slow})]{k_1} [C_{10}H_{17}N\cdot MoO_4]^{2-} \quad \ldots (2)$$

$$C_{10}H_{18}N^+ + MoO_4^{2-} \xrightarrow[(slow)]{k_2} [C_{10}H_{17}N\cdot MoO_4]^{2-} + H^+ \quad \ldots (3)$$

$$[C_{10}H_{17}N\cdot MoO_4]^{2-} + C_{10}H_{17}N + 2H_2O \xrightarrow[fast]{} H_2[(C_{10}H_{17}N)_2\, MoO_4] + 2OH^- \quad \ldots (4)$$

$$[C_{10}H_{17}N\cdot MoO_4]^{2-} + C_{10}H_{18}N^+ + H_2O \xrightarrow[fast]{} H_2[(C_{10}H_{17}N)_2\, MoO_4] + OH^- \quad \ldots (5)$$

Scheme 1

This mechanism leads to the rate expression,

$$\text{Rate} = \frac{[Mo]_t[Amn]_t\{k_1K_a + k_2[H^+]\}}{\{K_a + [H^+]\}} \quad \ldots (6)$$

where $[Mo]_t$ and $[Amn]_t$ represent the total concentrations of molybdate and amantadine respectively. Since the pK_a of amantadine is about 10.14, $K_a << [H^+]$ in the *p*H range employed and Eq. (6) may be written as,

$$\text{Rate} = \frac{[Mo]_t[Amn]_t\{k_1K_a + k_2[H^+]\}}{[H^+]} \quad \ldots (7)$$

or

$$\text{Rate} = [Mo]_t[Amn]_t\left\{\frac{k_1K_a}{[H^+]} + k_2\right\} \quad \ldots (8)$$

This rate equation explains all the observed orders in the tris buffers. The values of k_1 and k_2 computed from the slope and intercept of the initial rate versus $1/[H^+]$ plot, using a value of 7.2×10^{-11} mol dm^{-3} (refs 23 & 24) for K_a of amantadine, are $4.2 \pm 0.2 \times 10^{14}$ and $2.3 \pm 0.2 \times 10^{-2}$ dm^3 mol^{-1} s^{-1} respectively.

At *p*H 1.5, the initial rate of reaction was found to be negative even at a molybdate concentration of 1.0×10^{-4} mol dm^{-3}, but became progressively less negative when [amantadine] was increased in the range $2.1 - 10.7 \times 10^{-3}$ mol dm^{-3}, confirming that the rate determining step of interaction between amantadine and molybdate involved amantadine at *p*H 1.5 also. A plot of initial rate versus [amantadine] was found to be linear even at *p*H 1.5 (r = 0.994). However, unlike at *p*H 7.4, the plot obtained exhibited an intercept on rate axis. Such an intercept suggests a decrease in absorbance of molybdate even in the absence of amantadine and can be attributed to change in molybdate species due to its interaction with acid. Further, the initial rate of the reaction became more negative when [molybdate] was increased from $0.5\text{-}30.0 \times 10^{-5}$ mol dm^{-3}, probably for the same reason. In this case also a plot of initial rate versus [molybdate] was linear with an intercept on the rate axis (r = -0.999). The observed linear plots suggested that the reaction followed similar mechanism as at *p*H 7.4. In the *p*H range, 1.0-2.0, the rate of the reaction increased with increase in *p*H and a plot of initial rate versus $1/[H^+]$ was linear with an intercept (r = 0.999) in this range also. At *p*H 1.5, the rate of the reaction decreased with an increase in ionic strength, μ and a plot of log(initial rate) versus $\sqrt{\mu}$ was linear with negative slope of magnitude nearly unity (r = -0.998). In this *p*H range amantadine exists exclusively as a monoprotonated species, and molybdate exists as an equilibrium mixture of H_2MoO_4 and $HMoO_4^-$. The intercept on the rate axis of the initial rate versus $1/[H^+]$ plot suggests that both the species are reactive, while the increase in rate with decrease in acid concentration indicates that the monoanion was the preferred species. This may be due to ionic attraction between the positively charged amantadine and negatively charged monoprotonated molybdate ion. This observation is supported by the observed ionic strength effect. Thus, the mechanism of the reaction in acid medium may be given as shown in Scheme 2.

$$HMoO_4^- + H^+ \overset{K_2}{\Leftrightarrow} H_2MoO_4 \quad \ldots (9)$$

$$C_{10}H_{18}N^+ + HMoO_4^- \xrightarrow[\text{(slow)}]{k_3} [C_{10}H_{17}N\cdot MoO_4]^{2-} + 2H^+ \ldots (10)$$

$$C_{10}H_{18}N^+ + H_2MoO_4 \xrightarrow[\text{(slow)}]{k_4} [C_{10}H_{17}N\cdot MoO_4]^{2-} + 3H^+ \ldots (11)$$

$$[C_{10}H_{17}N\cdot MoO_4]^{2-} + C_{10}H_{18}N^+ + H_2O \xrightarrow[fast]{} H_2[(C_{10}H_{17}N)_2MoO_4] + OH^- \ldots (12)$$

Scheme 2

This mechanism leads to the rate expression,

$$\text{Rate} = \frac{[Mo]_t[Amn]_t\{k_3 + k_4K_2[H^+]\}}{\{1 + K_2[H^+]\}} \quad \ldots (13)$$

where $[Mo]_t$ and $[Amn]_t$ have the same significance as above. Since the logK_2 of molybdate can be computed to be 3.9 (ref. 14), in the *p*H range employed $K_2[H^+] >> 1$ and Eq. (12) may be written as,

$$\text{Rate} = \frac{[Mo]_t[Amn]_t\{k_3 + k_4K_2[H^+]\}}{K_2[H^+]} \quad \ldots (14)$$

or

$$\text{Rate} = [Mo]_t[Amn]_t\left\{\frac{k_3}{K_2[H^+]} + k_4\right\} \quad \ldots (15)$$

This rate equation again, explains all the observed orders in acid medium. The values of k_3 and k_4 computed from the slope and intercept of the initial rate versus $1/[H^+]$ plot using a value of 7.9×10^3 for K_2 (ref. 14) were $4.7 \pm 0.6 \times 10^{-1}$ and $1.5 \pm 0.2 \times 10^{-3}$ dm^3 mol^{-1} s^{-1} respectively.

Among the two reactive species of amantadine at *p*H 7.4, one would expect the monoprotonated species to be the preferred species if association of amantadine to molybdate is through hydrogen bonding and the opposite if coordination occurs. The

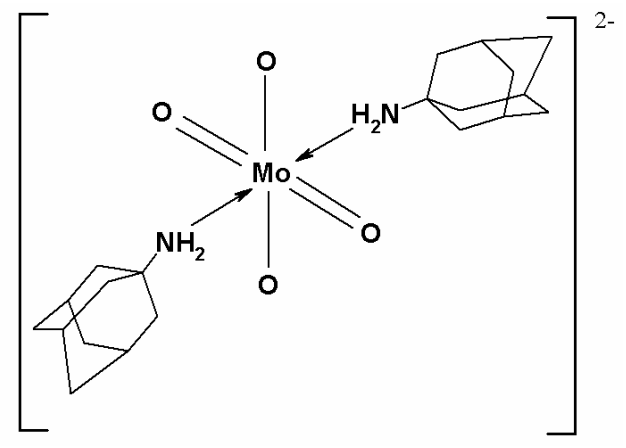

(I)

monoprotonated species may also be expected to be the preferred species in view of its unipositive charge and the dinegative nature of molybdate. However, the observed *p*H and ionic strength effects indicate that the preferred reactive species is the neutral amantadine species, in spite of its low concentration. This is understandable if the interaction is through direct coordination to the metal ion. Thus, the neutral species can coordinate much more easily to the metal ion than the monoprotonated species that requires deprotonation prior to coordination. Therefore the observed kinetic results are also in favour of direct coordination of amantadine to the metal ion and a consequent conversion of the tetrahedral molybdate to octahedral species. In acid medium the molybdate species are believed to be in octahedral geometry[16,25]. Again, the reaction between the diprotonated molybdate and the protonated amantadine in acid medium, can be expected to be less favourable if it were to occur through N–H--O hydrogen bridges. The observed results indicate that the rate of this reaction is comparable to that between the monoprotonated molybdate and the protonated amantadine ion, again suggesting direct coordination to the metal ion. We therefore assign an octahedral geometry to the prepared complex as shown in (**I**).

Thus it may be inferred that amantadine and sodium molybdate react at *p*H 1.5 as well as at *p*H 7.4 even at low concentrations of the drug and molybdate, hence, sodium molybdate supplements should be avoided while administering amantadine. Clinical studies are required for further confirmation of this fact.

Acknowledgement

One of the authors (NS) expresses her immense gratitude to Department of Science and Technology, Ministry of Science and Technology, New Delhi, India, for providing financial support to this work through DST-WOSA project scheme.

References

1 Stanicova J, Miskovsky P & Sutiak V, *Vet Med – Czech,* 46 (2001) 244.
2 Rajagopalan K, *Ann Rev Nutr,* 8 (1988) 401.
3 Abumrad N, Schneider A, Steel D & Rogers L, *Am J Clin Nutr,* 34 (1981) 2551.
4 http://lpi.oregonstate.edu/infocenter/minerals/molybdenum/.
5 Mustafa Ahmed A, Abdel-Fattah S A, Toubar Safaa S & Sultan Maha A, *J Anal Chem,* 59 (2004) 33; 140:187515CA.
6 Tang Wenxia, Qu Yun, Tai Anpang, Ji Xiujuan, Zhang Furong & Liu Li, *Nanjing Daxue Xuebao*, *Ziran Kexue*, 3 (1984) 471; 103:152569CA.
7 LIU Shu-Xia, Chun-Linga W G, YU Miaoa, LI Yu-Xinb & En-Boa W G, *Acta Chim Sinica,* 63 (2005) 1069.
8 Shu Xia Liu, Chun Mei Wang, Hong Ju Zhai, De Hui Li & En Bo Wang, *Chinese Chem Lett,* 15 (2004) 216.
9 Juan Li, Yanfei Qi, Enbo Wanga, Jing Li, Hongfang Wang, Yangguang Li, Ying Lu, Na Hao, Lin Xu & Changwen Hu, *J Coord Chem,* 57 (2004) 715.
10 William A Nugent & Richard L Harlow, *Inorg Chem,* 19 (1980) 777.
11 *The Merck Manual of Diagnosis and Therapy; Section 22, Clinical Pharmacology*, (Merck & Co Inc, New Jersey) 2006; http://www.merck.com/mrk.shared/mmanual/section22/chapter299/299a.jsp.
12 Shargel Leon, *Pharm Rev*, (John Wiley & Sons, New York) 1990.
13 Gringauz Alex, *Introduction to Medicinal Chemistry – How Drugs Act and Why,* (Wiley-VCH, New York) 1996.
14 Toru Ozeki & Hiroshi Kihara, *Anal Chem,* 60 (1988) 2055.
15 Aveston J, Anacker E W & James S Johnson, *Inorg Chem,* 3 (1964) 735.
16 Dan S Honig & Kenneth Kustin, *J Phys Chem,* 76 (1972) 1575.
17 *Japanese Pharmacopoeia*, 14th Edn, Part II, *Infrared reference spectra, amantadine hydrochloride*, p. 1093; http://jpdb.nihs.go.jp/jp14e/14data/Spectra_IR/1093.pdf.
18 Harvey P D, Gilson D F R & Butler I S, *J Phys Chem,* 91 (1987) 1267.
19 Nakamoto K, *Infrared and Raman Spectra of Inorganic and Coordination Compounds.* 5 Edn, (John Wiley and Sons, New York) 1997.
20 Foil A Miller & Charles H Wilkins, *Anal Chem,* 24 (1952) 1253.
21 Stanicova J, Kovalck P, Chinsky L & Miskovsky P, *Vib Spectrosc*, 25 (2001) 41.
22 Gandhi Ch S, Shuck K, Lear J D, Dieckmann G R, DeGrado, W F, Lamb R A & Pinto L H, *J Biol Chem*, 274 (1999) 5474.
23 Perrin D D & Hawkins I, *Experientia,* 28 (1972) 880.
24 Robert I Gelb & Daniel A Laufer, *J Chem Eng Data*, 28 (1983) 335.
25 Katharine Gilbert & Kenneth Kustin, *J Am Chem Soc,* 98 (1976) 5502.